

pH-Switchable Bioelectrocatalysis of Hydrogen Peroxide on Layer-by-Layer Films Assembled by Concanavalin A and Horseradish Peroxidase with Electroactive Mediator in Solution

Huiqin Yao^{†,‡} and Naifei Hu^{*,†}

Department of Chemistry, Beijing Normal University, Beijing 100875, People's Republic of China, and
Department of Chemistry, Ningxia Medical University, Yinchuan 750004, People's Republic of China

Received: December 28, 2009; Revised Manuscript Received: February 1, 2010

The lectin protein concanavalin A (Con A) and the glycoenzyme horseradish peroxidase (HRP) were assembled into {Con A/HRP}_n layer-by-layer films on electrodes mainly by biospecific affinity between them. The cyclic voltammetric (CV) response of ferricyanide (Fe(CN)₆^{3−}) at {Con A/HRP}_n film electrodes was very sensitive to the environmental pH. The peak currents of Fe(CN)₆^{3−} were quite large at pH 4.0 but greatly suppressed at pH 9.0, demonstrating reversible pH-sensitive “on–off” behavior. This property could be used to realize pH-controlled electrochemical reduction of H₂O₂ catalyzed by HRP immobilized in {Con A/HRP}_n films and mediated by Fe(CN)₆^{3−} in solution. The modulation of the solution pH was also realized by in situ biochemical reactions with various enzymes in solution and was used to tune the pH-switchable bioelectrocatalysis. The possible mechanism of the pH-responsive on–off behavior of the films toward the probe was explored, and the electrostatic interaction between the films and the probe is believed to play a key role in deciding the pH-sensitive behavior of the films. This “smart” interface may be used to establish a foundation for fabricating novel pH-controllable electrochemical biosensors based on bioelectrocatalysis with immobilized enzymes.

Introduction

The research on the electrochemistry of redox enzymes may provide a working model for the mechanistic study of enzyme-catalyzed reactions in real biological systems, and the bioelectrocatalysis based on the direct or mediated electrochemistry of enzymes can establish a foundation for fabricating biosensors and bioreactors.^{1–3} The electrochemistry involving enzymes has thus attracted increasing attention among researchers in recent years. However, one of the major challenges in this course is to develop the controllable or “stimuli-responsive” bioelectrocatalysis, which is of great significance in the study of switchable biosensors, bioelectronic devices, signal amplification, biofuel cells, and information processing.^{4–6} Particularly, the pH-switchable bioelectrocatalysis with enzymes has aroused great interest lately.^{7–9} For example, Katz and co-workers prepared a modified electrode with a poly(4-vinyl pyridine) brush functionalized with Os complex redox groups and applied the films to electrochemically oxidize glucose catalyzed by glucose oxidase (GOD) in solution and mediated by Os complex units in the films.⁷ The films exhibited a pH-sensitive structure change and could be used to reversibly activate/deactivate the bioelectrocatalysis of glucose by changing the solution pH. Recently, we found that the {Con A/Dex}_n layer-by-layer (LbL) films assembled by concanavalin A (Con A) and dextran (Dex) on the electrode surface showed a reversible pH-controlled bioelectrocatalysis.⁹ The pH-sensitive on–off electrocatalytic reduction of H₂O₂ by horseradish peroxidase (HRP) with Fe(CN)₆^{3−} as the diffusional electron-transfer mediator and electrocatalytic oxidation of glucose by GOD mediated by ferrocenedicarboxylic acid (Fc(COOH)₂) were realized. How-

ever, one obvious shortcoming of the above systems was that all of the enzymes used were in the solution phase but not immobilized in the films. As is well-known, the enzymes dissolved in solution cannot be used efficiently in bioelectrocatalysis, and they are difficult to recover and reuse. Particularly, the enzyme immobilization is usually one necessary step in fabricating biosensors, and the immobilization can significantly strengthen the stability of the enzymes.^{10,11} Therefore, the effective immobilization of enzymes on the electrode surface without altering their structure and bioactivity is highly desired for development of electrochemical biosensors and other biodevices.

There is a variety of methods to immobilize enzymes, including physical entrapment, surface adsorption, sol–gel encapsulation, covalent bonding, and LbL assembly. Among them, the LbL assembly technique, which was first developed by Decher in the 1990s,¹² has demonstrated rapid development in recent years. Over other immobilization methods, the LbL assembly displays distinguished advantages in the precise control of film thickness at a nanometer scale according to a predesigned architecture and in its simple procedure and high versatility in the assembly.^{12–14} The building blocks of LbL assembly were originally just polyelectrolytes but now have been extended to other species including enzymes and proteins.¹⁴ For example, some redox proteins or enzymes have been immobilized on the electrode surface by LbL assembly, and the electrochemistry and electrocatalysis based on the proteins have been developed.^{15–17}

In constructing enzyme LbL films, the driving force is usually electrostatic interaction, but nonelectrostatic interactions such as hydrogen bonding and biospecific recognition have also been used.¹³ Herein, the biospecific recognition includes enzyme–substrate, antibody–antigen, avidin–biotin, and lectin–sugar interactions,^{14,18–20} and the lectin–sugar interaction has attracted

* To whom correspondence should be addressed. E-mail: hunaifei@bnu.edu.cn. Tel: (+86) 10-5880-5498. Fax: (+86) 10-5880-2075.

[†] Beijing Normal University.

[‡] Ningxia Medical University.

increasing attention currently. Con A is the best-known member of the lectin proteins and exists as a tetramer at neutral pH. The most characteristic feature of Con A is that each of its subunits contains a binding site to some specific sugar groups such as glucose and mannose, forming a highly specific Con A–sugar complex.^{21–23} The glycoenzyme HRP contains lots of mannose residues on their surface,²⁴ Con A and HRP can thus be assembled into LbL films by the biospecific lectin–sugar affinity between them, designated as {Con A/HRP}_n.^{23–27} Particularly, the {Con A/HRP}_n films assembled on electrodes have been used as electrochemical biosensors for H₂O₂ determination through the biocatalytic activity of HRP.^{23,28} However, pH-controlled bioelectrocatalysis with {Con A/HRP}_n LbL films has not been reported. In general, while the pH-responsive LbL films have been studied extensively and applied in different fields,^{29–32} the pH-controllable bioelectrocatalysis with LbL films has received only limited attention.⁹ In particular, to the best of our knowledge, no study on the pH-switchable bioelectrocatalysis with the enzyme immobilized in LbL films has been reported up to now.

In the present work, {Con A/HRP}_n LbL films were assembled on pyrolytic graphite (PG) electrodes and used to immobilize HRP. The films demonstrated a pH-sensitive on–off property toward the electroactive probe Fe(CN)₆^{3–} in its electrochemical responses. At pH 4.0, the films were permeable toward the probe, and the cyclic voltammetric (CV) response of the probe was quite large, while at pH 9.0, the films became impermeable to the probe, and the CV response of the probe was greatly suppressed. This pH-sensitive switching property of the films was further used to control or modulate the electrochemical reduction of hydrogen peroxide (H₂O₂) catalyzed by HRP immobilized in the films with Fe(CN)₆^{3–} as the mediator in solution. The sensing of H₂O₂ is of great importance in many fields, including the food industry, environmental monitoring, and clinical diagnosis. Moreover, H₂O₂ is the product of many biological reactions with various oxidases.³³ This work not only provides a foundation for fabricating electrochemical biosensors to make determination of H₂O₂ but also offers the opportunity to control or switch the bioelectrocatalysis by changing the surrounding pH. In addition, most of the pH-switchable films are activated/deactivated by artificial addition of dilute NaOH/HCl into the reaction solution, but the various pH-sensitive physiological processes in real biological systems are controlled by different biochemical reactions, which can change the pH of the system.³⁴ It is thus necessary to combine the pH-switchable bioelectrocatalytic system with the environment controlled by in situ biochemical reactions.^{8,35–37} In the present work, the surrounding pH was modulated by in situ enzyme-catalyzed reactions and then used to switch the bioelectrocatalytic reduction of H₂O₂ with the {Con A/HRP}_n film system coupled by Fe(CN)₆^{3–} in solution. Furthermore, the mechanism of the pH-dependent permeability of the films toward the probe was explored and discussed and believed to be mainly attributed to the electrostatic interaction between the films and the probe. The better understanding of the essence of interactions in this pH-sensitive smart model interface may open a general way to design a novel type of pH-controllable biosensors based on the bioelectrocatalysis with immobilized enzymes.

Experimental Section

1. Reagents. Chitosan (CS, the degree of deacetylation is more than 85%, MW ≈ 200 000), concanavalin A extracted from Jack beans (Con A, type V, MW ≈ 104 000), horseradish

peroxidase (HRP, E.C. 1.11.1.7, type II, MW ≈ 44 000, 250 000 units g^{–1}), esterase from porcine liver (Est, 17 000 units g^{–1}), urease from Jack beans (Ur, E.C. 3.5.1.5, type III, 39 290 units g^{–1}), ferrocenemethanol (FcOH), hexaammineruthenium(III) chloride (Ru(NH₃)₆Cl₃), 3-mercapto-1-propanesulfonate (MPS, 90%), and tris(hydroxymethyl) aminomethane (Tris) were purchased from Sigma–Aldrich. Potassium ferricyanide (K₃Fe(CN)₆), potassium ferrocyanide (K₄Fe(CN)₆), urea, and hydrogen peroxide (H₂O₂, 30%) were obtained from Beijing Chemical Engineering Plant. The dilute H₂O₂ aqueous solutions were freshly prepared before being used. Ethyl butyrate (EB) was from Tianjin Bodi Chemical Engineering. All other reagents were of analytical grade. Britton–Robinson buffers at pH 3.0–10.0 contained 0.1 M NaCl, and the pH was adjusted to the desired value with dilute HCl or NaOH solutions. Tris–HCl buffers (0.1 M) at pH 7.4 containing 0.1 M NaCl, 1 mM MnCl₂, and 1 mM CaCl₂ were used to prepare Con A and HRP solutions.³⁸ All solutions were prepared with water purified twice by ion exchange and subsequent distillation.

2. Film Assembly. Prior to assembly, basal plane pyrolytic graphite (PG, Advanced Ceramics, geometric area 0.16 cm²) disk electrodes were abraded on 320 grit metallographic sandpaper while flushing with water. After being ultrasonicated in water for 30 s and dried in air, the electrodes were first immersed in 1 mg mL^{–1} CS solutions at pH 5.0 for 30 min, forming a CS precursor layer on PG surface. The PG/CS electrodes were then alternately immersed into Con A (1 mg mL^{–1}, pH 7.4) and HRP (1 mg mL^{–1}, pH 7.4) aqueous solutions for 30 min each, with intermediate water rinsing and air stream drying, until the desired number of bilayers (*n*) was obtained, forming {Con A/HRP}_n LbL films on the PG/CS surface.

For the quartz crystal microbalance (QCM) study, gold-coated quartz crystal resonator electrodes (International Crystal Manufacturing Co.) were first covered by a few drops of a freshly prepared “piranha” solution (3:7 volume ratio of 30% H₂O₂ and concentrated H₂SO₄). Caution: the piranha solution should be handled with extreme care, and only a small volume should be prepared at any time) on each side for 10 min and then washed thoroughly with water and ethanol successively. The QCM gold electrodes were then immersed in 4 mM MPS ethanol solutions for 24 h to chemisorb an MPS monolayer on the gold surface by formation of a Au–S bond between Au and MPS, introducing negative charges on the surface. The CS precursor layer and following {Con A/HRP}_n LbL films were then assembled on the Au/MPS surface in the same way as on the PG electrodes.

3. In Situ pH Modulation by Enzyme-Catalyzed Reactions. For the experiments of enzyme reaction-induced pH modulation, the unbuffered solution initially contained 0.1 M NaCl, 5 units mL^{–1} Est, and 15 units mL^{–1} Ur with the solution pH at about 6.5. When EB was slowly added into the solution with a concentration of 10 mM under magnetic stirring, butyric acid was produced by Est enzymatic reaction, resulting in the lowering of the solution pH. The solution pH reached the steady state of approximately 4.0 in about 10 min. When urea was slowly added into this pH 4.0 solution with a concentration of 6 mM, ammonia was produced by enzymatic catalysis with Ur, leading to the increase of the solution pH. The pH reached the steady value of approximately 9.0 in about 30 min. This procedure could be repeated several times so that the solution pH could be switched between pH 4.0 and 9.0 by in situ biocatalysis. This kind of solution was also used to test the pH-sensitive on–off bioelectrocatalytic behavior of {Con A/HRP}_n films in the presence of Fe(CN)₆^{3–} and H₂O₂ in solution.

4. Apparatus and Procedures. A CHI 660A or 621B electrochemical workstation (CH Instruments) was used for electrochemical measurements. A typical three-electrode cell was used with a saturated calomel electrode (SCE) as the reference, a platinum foil as the counter, and a PG electrode with films as the working electrode. Before electrochemical measurements, the electrolyte solutions were purged with high-purity nitrogen for at least 10 min. The nitrogen atmosphere was then kept for the entire experiment. Electrochemical impedance spectroscopy (EIS) measurements were performed in 1:1 $\text{K}_4\text{Fe}(\text{CN})_6/\text{K}_3\text{Fe}(\text{CN})_6$ mixture solutions with a total concentration of 5 mM, and a sinusoidal potential modulation with an amplitude of ± 5 mV and frequency from 10^5 –0.1 Hz was superimposed on the formal potential of the $\text{Fe}(\text{CN})_6^{4-/3-}$ redox couple at 0.17 V versus SCE.

The pH measurements were performed with a PHSJ-3F pH meter (Shanghai Precision & Scientific Instruments).

QCM was carried out with a CHI 420 electrochemical analyzer (CH Instruments). The quartz crystal resonator (AT-cut) had a fundamental resonance frequency of 8 MHz and was covered by thin gold films on both sides (geometric area 0.196 cm^2 per one side). After each adsorption step, the QCM gold electrodes were washed thoroughly in water for about 30 s and dried under a nitrogen stream, and the frequency change was then measured in air by QCM.

Scanning electron microscopy (SEM) was performed using an S-4800 scanning electron microscope (Hitachi) with an acceleration voltage of 3 kV. The $\text{CS}/\{\text{Con A}/\text{HRP}\}_5$ films assembled on the MPS-modified QCM gold electrodes were used as the sample. Before the SEM imaging, the surface of the samples was coated by thin Pt films with an E-1045 sputtering coater (Hitachi).

All experiments were performed at an ambient temperature of 20 ± 2 °C.

Results and Discussion

1. Assembly of $\{\text{Con A}/\text{HRP}\}_n$ LbL Films. With its pK_a at about 6.5,³⁹ CS carries positive charges at pH 5.0 and can be adsorbed on the negatively charged PG surface.⁴⁰ Con A carries net negative surface charges at pH 7.4 due to its pI at about 5.0⁴¹ and thus can be adsorbed on an oppositely charged PG/CS surface by electrostatic attraction. As the best-known lectin protein, Con A possesses strong biospecific affinity with glycoenzyme HRP,^{23–28} and the $\{\text{Con A}/\text{HRP}\}_n$ LbL films can thus be assembled on a PG/CS surface mainly by the biospecific interaction between Con A and mannose residues intrinsically existing on the surface of HRP. At pH 7.4, Con A carries net negative surface charges,⁴¹ and HRP shows positive charges with its pI at 8.9;⁴² the electrostatic interaction between them may also play a role in the assembly of the films.

The growth of $\{\text{Con A}/\text{HRP}\}_n$ multilayer films on a PG/CS surface was first monitored and confirmed by the direct electrochemical response of HRP (Figure 1A). After each adsorption cycle creating a new Con A/HRP bilayer on the PG/CS electrode surface, the film electrode was transferred into pH 7.4 buffers containing no HRP and tested by CV between +0.1 and -0.8 V. A pair of well-defined and nearly reversible peaks was observed at approximately -0.33 V versus SCE, characteristic of the $\text{Fe}(\text{III})/\text{Fe}(\text{II})$ redox couple of the HRP heme prosthetic group.^{43,44} The reduction peak currents increased linearly with scan rates from 0.05 to 2.0 V s^{-1} , suggesting that the voltammetric behavior of HRP in the films is diffusionless and surface-confined. In this case, integration of the CV reduction peak would give the charge (Q) value for full reduction

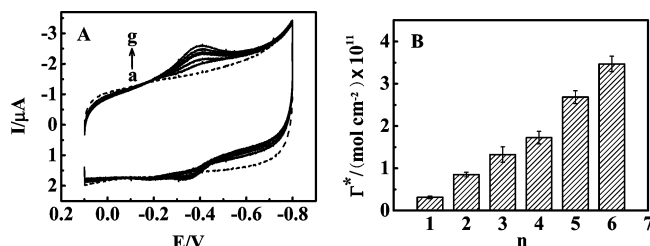


Figure 1. (A) CVs in pH 7.4 buffers at 0.2 V s^{-1} for $\{\text{Con A}/\text{HRP}\}_n$ films assembled on a PG/CS electrode. The number of bilayers (n): (a) 0, (b) 1, (c) 2, (d) 3, (e) 4, (f) 5, (g) 6. (B) Dependence of the surface concentration of electroactive HRP (Γ^*) on n for $\{\text{Con A}/\text{HRP}\}_n$ films.

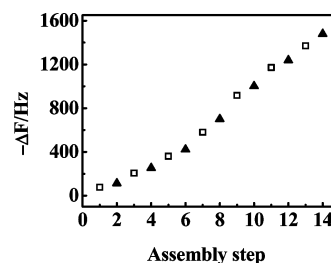


Figure 2. QCM frequency shift ($-\Delta F$) with assembly step for assembly of $\{\text{Con A}/\text{HRP}\}_n$ LbL films on a Au/MPS/CS surface; Con A (\square) and HRP (\blacktriangle) adsorption steps.

of all electroactive HRP in the films, which could be further converted to the surface concentration of electroactive HRP (Γ^* , mol cm^{-2}) in the films through the Faraday's law.⁴⁵ Γ^* increased with the number of bilayers (n) at least up to 6 (Figure 1B), indicating that the $\{\text{Con A}/\text{HRP}\}_n$ LbL films are successfully assembled on PG/CS surface.

CV and EIS with $\text{Fe}(\text{CN})_6^{3-/4-}$ as the electroactive probe were also used to confirm the assembly of $\{\text{Con A}/\text{HRP}\}_n$ LbL films on a PG/CS surface, and the detailed results are presented in Supporting Information Figures S1 and S2.

The growth of $\{\text{Con A}/\text{HRP}\}_n$ LbL films was further confirmed by QCM. The QCM frequency decrease ($-\Delta F$) usually reflects the mass increase on QCM gold electrodes. The QCM results showed that the $-\Delta F$ value had a roughly linear relationship with adsorption step in the assembly of $\{\text{Con A}/\text{HRP}\}_n$ films (Figure 2), suggesting that the films are successfully fabricated on the Au/MPS/CS surface and the building up of the films is in a roughly reproducible manner.

2. pH-Sensitive CV Behavior of $\text{Fe}(\text{CN})_6^{3-}$ at $\{\text{Con A}/\text{HRP}\}_5$ Film Electrodes. The CV behavior of $\text{Fe}(\text{CN})_6^{3-}$ at $\{\text{Con A}/\text{HRP}\}_5$ film electrodes with $n = 5$ was very sensitive to the pH of $\text{Fe}(\text{CN})_6^{3-}$ solutions (Figure 3A). For example, at pH 4.0, $\text{Fe}(\text{CN})_6^{3-}$ showed relatively large CV reduction peak current (I_{pc}) and quite small peak separation (ΔE_p). However, at pH 9.0, the I_{pc} decreased drastically, accompanied by the increase of peak separation ΔE_p (Figure 3B). From pH 4.0 to 9.0, the I_{pc} and ΔE_p experienced a dramatic change. Particularly, when $\text{pH} \geq 9.0$, the CV signal of $\text{Fe}(\text{CN})_6^{3-}$ could hardly be observed. This pH-sensitive CV behavior of $\text{Fe}(\text{CN})_6^{3-}$ should not be attributed to the property of the probe itself since the CV behavior of $\text{Fe}(\text{CN})_6^{3-}$ at bare PG electrodes was essentially pH-independent. It thus must be related to the interaction between the probe and the films.

The pH-dependent CV behavior of the probe for $\{\text{Con A}/\text{HRP}\}_5$ films inspired us to use the system as a pH-sensitive switch. According to Figure 3, two typical pH values, pH 4.0 and 9.0, were selected in the following studies. In pH 4.0 buffers, the films were in the on state, and the probe showed a nearly

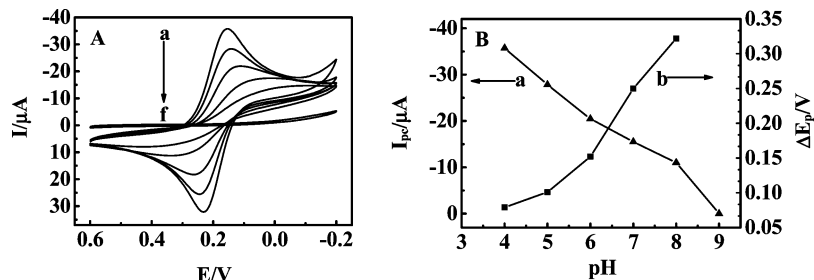


Figure 3. (A) CVs of 1 mM $\text{K}_3\text{Fe}(\text{CN})_6$ at 0.1 V s^{-1} for $\{\text{Con A/HRP}\}_5$ films in buffers at pH (a) 4.0, (b) 5.0, (c) 6.0, (d) 7.0, (e) 8.0, and (f) 9.0. (B) Influence of solution pH on the (a) CV reduction peak current (I_{pc}) and (b) peak separation (ΔE_{p}).

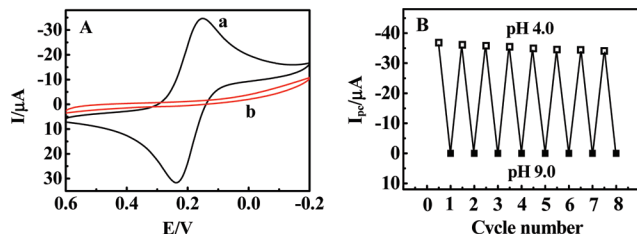


Figure 4. (A) CVs of 1 mM $\text{K}_3\text{Fe}(\text{CN})_6$ at 0.1 V s^{-1} for $\{\text{Con A/HRP}\}_5$ films in buffers at pH (a) 4.0 and (b) 9.0. (B) Dependence of the CV reduction peak current (I_{pc}) of $\text{K}_3\text{Fe}(\text{CN})_6$ on the cycle number when the solution pH switched between pH 4.0 (\square) and 9.0 (\blacksquare) for the same $\{\text{Con A/HRP}\}_5$ films.

reversible CV peak pair with quite large peak currents (Figure 4A, curve a), while in pH 9.0 solutions, the films were in the off state, and the CV response of $\text{Fe}(\text{CN})_6^{3-}$ was significantly suppressed and even could hardly be observed (Figure 4A, curve b). This on–off property of the system with pH was quite reversible. By switching the film electrode in buffers between pH 4.0 and 9.0, the corresponding CV responses switched between the on and off states (Figure 4B), and this on–off behavior could be repeated at least for 10 cycles.

The pI of Con A is about 5.0,⁴¹ and the pI of HRP is 8.9.⁴² Therefore, at pH 4.0, the $\{\text{Con A/HRP}\}_5$ films would carry net positive charges and have a strong electrostatic attraction with negatively charged $\text{Fe}(\text{CN})_6^{3-}$ in solution. This would make the probe go through the films more easily, leading to the quite large CV response of the probe. In contrast, at pH 9.0, the films would carry net negative charges and have a strong electrostatic repulsion with the probe. This might hinder the probe from entering the films and limit the electron exchange of the probe with underlying electrodes, thus resulting in the very small CV signal. The pH-sensitive behavior of $\{\text{Con A/HRP}\}_n$ films toward $\text{Fe}(\text{CN})_6^{3-}$ is therefore most probably attributed to the electrostatic interaction between the films and the probe.

At pH 4.0, while both Con A and HRP are positively charged, the $\{\text{Con A/HRP}\}_n$ films should be stable because the main interaction between Con A and HRP is the lectin–sugar biospecific interaction, which would overcome the electrostatic repulsion between the similarly charged species. To examine the film stability, the $\{\text{Con A/HRP}\}_5$ films were stored in pH 4.0 blank buffers for most of the storage time and placed in $\text{Fe}(\text{CN})_6^{3-}$ solutions at pH 4.0 for CV testing occasionally. During one week of storage, the peak potentials of the probe maintained the same position, and the reduction peak current increased by only about 8% of their initial value, suggesting that the $\{\text{Con A/HRP}\}_5$ films are quite stable in pH 4.0 solutions.

The pH-responsive switching behavior of $\{\text{Con A/HRP}\}_5$ films toward the $\text{Fe}(\text{CN})_6^{3-/4-}$ redox probe was also observed by EIS (Supporting Information Figure S3A). In pH 4.0 buffers, the EIS response in the form of a Nyquist diagram showed a

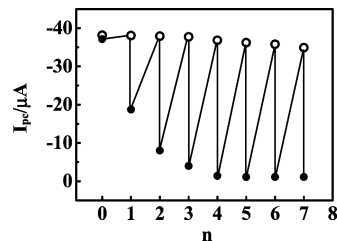


Figure 5. Influence of the number of bilayers (n) of $\{\text{Con A/HRP}\}_n$ films on the CV reduction peak current (I_{pc}) of 1 mM $\text{K}_3\text{Fe}(\text{CN})_6$ in buffers at pH 4.0 (\circ) and 9.0 (\bullet) at 0.1 V s^{-1} .

Warburg line with no obvious semicircle in the high-frequency domain, indicating that the charge-transfer resistance (R_{ct}) of the system is very small. At pH 9.0, however, a large semicircle was observed, reflecting the considerably high R_{ct} value for the system. This pH-sensitive on–off behavior of EIS was reversible and could be repeated for several cycles between pH 4.0 and 9.0 (Supporting Information Figure S3B).

3. Influencing Factors. Further studies showed that the outermost layer of the films had little influence on the pH-dependent CV behavior of $\text{Fe}(\text{CN})_6^{3-}$. For example, at pH 4.0, $\text{Fe}(\text{CN})_6^{3-}$ demonstrated the identical CVs for both $\{\text{Con A/HRP}\}_5$ and $\{\text{Con A/HRP}\}_4/\text{Con A}$ films with quite large peak heights, while at pH 9.0, both films were “closed” for the probe (Supporting Information Figure S4). These results suggest that the interpenetration between neighboring Con A and HRP layers may happen in the film assembly, which is a common phenomenon in LbL assembly.¹² According to the dimensions of the HRP molecule ($6.0 \times 3.5 \times 3.0 \text{ nm}^3$),⁴⁶ the average area occupied by one HRP molecule would be about 16.5 nm^2 , which was equivalent to $1.0 \times 10^{-11} \text{ mol cm}^{-2}$ for the surface concentration of HRP in monolayer adsorption if assuming that the HRP molecules were packed compactly. The average surface concentration of electroactive HRP (Γ^*) for each Con A/HRP bilayer estimated by CV experiments was about $5.8 \times 10^{-12} \text{ mol cm}^{-2}$ (Figure 1B), only about 58% of the theoretical value. This implies that if all HRP molecules are electroactive, the arrangement of HRP molecules in its adsorption layer is quite loose and the interlayer mixing or penetrating would happen between the Con A and HRP layers in the assembly.

The number of bilayers (n) or the thickness of $\{\text{Con A/HRP}\}_n$ films showed considerable influence on the pH-dependent on–off CV property of the films toward $\text{Fe}(\text{CN})_6^{3-}$ (Figure 5). At pH 4.0, the CV reduction peak current (I_{pc}) of the probe showed little change with n , suggesting that at this pH, the permeability of the films toward the probe does not become poorer when the films become thicker. However, in pH 9.0 solutions, the I_{pc} value decreased dramatically with n from 1 to 4 and then tended to reach 0. With $n = 1$, $\text{Fe}(\text{CN})_6^{3-}$ showed a quite large CV response at pH 9.0 for the films, indicating that the very thin films could not be completely closed toward

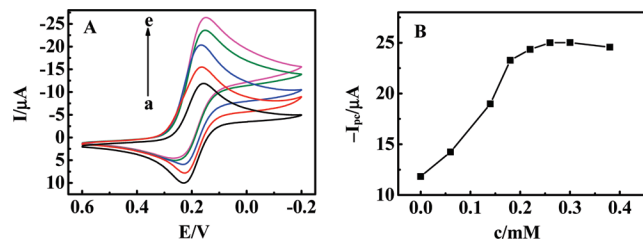
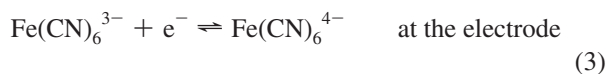
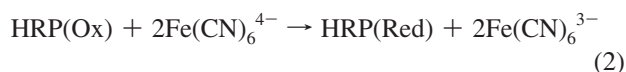
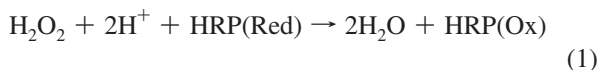


Figure 6. (A) CVs of {Con A/HRP}₅ films at 0.01 V s⁻¹ in pH 4.0 buffers containing 1 mM K₃Fe(CN)₆ and H₂O₂ at (a) 0, (b) 0.06, (c) 0.14, (d) 0.18, and (e) 0.26 mM. (B) Dependence of the CV electrocatalytic reduction peak current (*I*_{pc}) on the concentration of H₂O₂.

the probe. This is probably due to the relatively small amounts of negative charges for only one Con A/HRP bilayer at pH 9.0, which limits its electrostatic repulsion with Fe(CN)₆³⁻. Moreover, one Con A/HRP bilayer may not completely cover the PG/CS surface; some underlying CS layer with positive charges may be exposed and tend to attract Fe(CN)₆³⁻. With an increase of the *n* value, the *I*_{pc} decreased dramatically at pH 9.0. This should be mainly ascribed to the larger amounts of negative charges in the thicker films and the corresponding stronger electrostatic repulsion between the films and the probe. In addition, more bilayers would completely cover the electrode surface. Considering that the {Con A/HRP}₅ films demonstrated the most pronounced difference in *I*_{pc} values between pH 4.0 and 9.0, the films with *n* = 5 were selected in the present work.

4. pH-Controlled Bioelectrocatalytic Reduction of H₂O₂ by {Con A/HRP}_{*n*} Films with Fe(CN)₆³⁻ as the Mediator. The pH-responsive switching property of {Con A/HRP}₅ films toward Fe(CN)₆³⁻ in CV could be used to control or modulate electrocatalytic reduction of H₂O₂. When H₂O₂ was added into the Fe(CN)₆³⁻ solution at pH 4.0, in comparison with the system in the absence of H₂O₂, the CV reduction peak of Fe(CN)₆³⁻ for {Con A/HRP}₅ films increased dramatically, accompanied by the decrease of the oxidation peak (Figure 6A). The electrocatalytic reduction peak current (*I*_{pc}) increased initially with the concentration of H₂O₂ in solution in the range of 0.05–0.26 mM and then tended to level off (Figure 6B). All of these are characteristic of electrochemical reduction of H₂O₂ catalyzed by HRP and mediated by Fe(CN)₆³⁻, and the mechanism can be expressed by the following equations^{47–49}



where HRP(Red) stands for the HRP–Fe(III) form and HRP(Ox) usually represents the radical intermediate with oxidation state +5, known as compound I.⁵⁰

However, when {Con A/HRP}₅ films were placed in pH 9.0 buffers containing the same amount of Fe(CN)₆³⁻ and H₂O₂, the electrocatalytic response became quite small or even could hardly be observed (Figure 7A, curve b). This is because the films become off toward Fe(CN)₆³⁻ at pH 9.0, resulting in the interruption of the catalytic cycle. Therefore, the bioelectro-

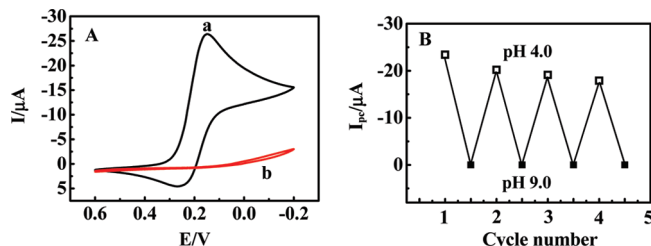
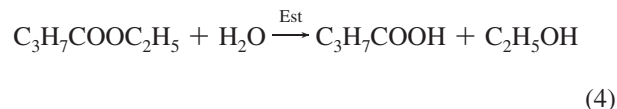


Figure 7. (A) CVs of {Con A/HRP}₅ films at 0.01 V s⁻¹ in buffers containing 1 mM K₃Fe(CN)₆ and 0.26 mM H₂O₂ at pH (a) 4.0 and (b) 9.0. (B) Dependence of the CV electrocatalytic reduction peak current (*I*_{pc}) on solution pH switched between pH 4.0 (□) and 9.0 (■) for the same {Con A/HRP}₅ films.

catalytic reduction of H₂O₂ could be switched by the different permeability of {Con A/HRP}₅ films toward Fe(CN)₆³⁻ at different pHs. The bioelectrocatalysis is in the on state at pH 4.0 and in the off state at pH 9.0. This pH-sensitive switching bioelectrocatalysis was also reversible, and the on–off behavior for the films could be repeated for at least several cycles between pH 4.0 and 9.0, although the *I*_{pc} at pH 4.0 showed a small decreasing trend with the number of cycles (Figure 7B). In addition, the CV reduction peak current ratio, *I*_{pc4}/*I*_{pc9}, could be amplified by the bioelectrocatalysis, where *I*_{pc4} and *I*_{pc9} were CV reduction peak currents at pH 4.0 and 9.0 for the same {Con A/HRP}₅ films, respectively. In solutions containing only Fe(CN)₆³⁻, the *I*_{pc4}/*I*_{pc9} ratio was about 11, while in solutions containing both Fe(CN)₆³⁻ and H₂O₂, the ratio increased to about 26.

5. In Situ pH Modulation by Enzyme-Catalyzed Reactions and Corresponding Bioelectrocatalysis. The solution pH can be controlled not only by external addition of dilute NaOH or HCl solutions but also by in situ enzyme-catalyzed reactions.^{8,35–37} This latter pH-modulation approach combined with the pH-sensitive switching bioelectrocatalysis for the {Con A/HRP}₅–Fe(CN)₆³⁻–H₂O₂ system may provide a model to realize pH-switchable bioelectrocatalytic reduction of H₂O₂ through biochemical control. In the present work, two enzymes, Est and Ur, were used to catalyze the hydrolysis reactions of EB and urea, respectively, and the corresponding reactions can be expressed by the following equations^{51–53}



The pH of unbuffered solutions containing Est and Ur was about 6.5. When EB was added into the solution, butyric acid (C₃H₇COOH) was produced (eq 4), making the solution pH decrease and reach the steady state at pH 4.0 in about 10 min. After urea was added into this pH 4.0 solution, ammonia was produced (eq 5), leading to the increase of the solution pH until pH 9.0 in 30 min. This pH-change profile with time is demonstrated in Figure 8. The in situ pH modulation by enzyme-catalyzed reactions could be repeated several cycles by alternate addition of EB and urea in the enzyme solution, and the solution pH could be switched between 4.0 and 9.0. Moreover, the period of time during which the solution reached the steady pH depended on the concentrations of substrates (Supporting

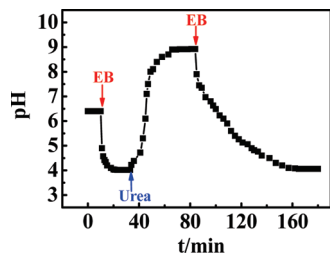


Figure 8. Time-dependent pH changes induced by in situ enzyme-catalyzed reactions upon addition of EB and urea. The detailed procedure is given in Experimental Section.

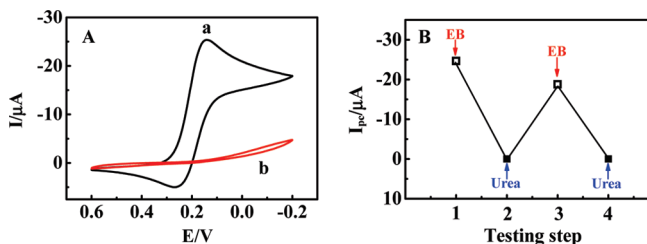


Figure 9. (A) CVs of {Con A/HRP}₅ films at 0.01 V s⁻¹ in unbuffered solutions containing 5 units mL⁻¹ Est, 15 units mL⁻¹ Ur, 1 mM K₃Fe(CN)₆, and 0.25 mM H₂O₂. (a) After 10 min of reaction with the addition of 10 mM EB. (b) After subsequent 30 min of reaction with the addition of 6 mM urea. (B) Dependence of the CV catalytic reduction peak current (*I*_{pc}) on alternate addition of EB (□) and urea (■) solutions for the same {Con A/HRP}₅ films.

Information Figure S5). More concentrated EB and urea solutions added into the enzyme solution would lead to the shorter period of time for the solution to reach the desired pH.

The in situ pH modulation by enzyme-catalyzed reactions could also be used to control pH-sensitive on–off bioelectrocatalysis of H₂O₂ for the {Con A/HRP}₅ films coupled with Fe(CN)₆³⁻ in solution. The films were first placed in unbuffered solutions containing Est, Ur, Fe(CN)₆³⁻, and H₂O₂ with the pH at about 6.5. After EB was added, the solution pH decreased and finally reached 4.0. The CV was performed, and a quite large electrocatalytic reduction peak was observed (Figure 9A, curve a). The urea solution was then added into the solution, making the solution pH increase up to 9.0. The CV was run again, but the signal was significantly suppressed (Figure 9A, curve b). The on–off behavior could be repeated several times (Figure 9B). All of these results were very similar to those of Figure 7, where the pH was tuned by external addition of dilute NaOH or HCl solutions.

6. Possible Mechanism of the pH-Sensitive Switching Behavior of {Con A/HRP}₅ Films toward Fe(CN)₆³⁻. There are two typical kinds of mechanism for the pH-sensitive permeation behavior of polyelectrolyte films toward probes. One is the structure change of films induced by environmental pH, for which the porosity or swelling property of the films is pH-sensitive.^{7,8,15,54,55} Another is controlled by the electrostatic interaction between probes and films, where the net film charge is switched by external pH.^{9,29,31,32,56}

According to the discussion in subsection 2, the pH-sensitive switching CV behavior of {Con A/HRP}₅ films toward Fe(CN)₆³⁻ is most probably attributed to the second mechanism. To support this speculation, the possible change of the surface morphology of {Con A/HRP}₅ films with solution pH was examined and compared by SEM after the films were immersed in buffers at different pHs for 10 min (Supporting Information Figure S6). With the same magnification, the films that had been immersed in pH 4.0 buffers showed the surface morphology

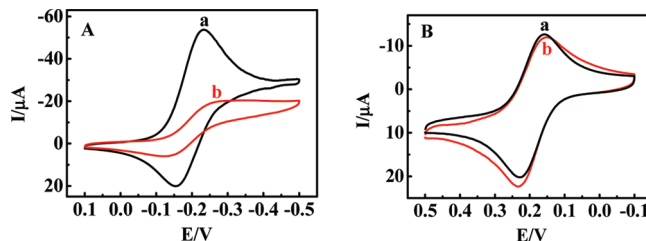


Figure 10. (A) CVs of 1 mM Ru(NH₃)₆Cl₃ at 0.1 V s⁻¹ for {Con A/HRP}₅ films in buffers at pH (a) 9.0 and (b) 4.0. (B) CVs of 0.5 mM FcOH at 0.1 V s⁻¹ for {Con A/HRP}₅ films in buffers at pH (a) 4.0 and (b) 9.0.

and roughness to be essentially the same as those in pH 9.0 buffers, indicating that the solution pH has no substantial influence on the structure of {Con A/HRP}₅ films, and the porosity of the films is not sensitive to the solution pH at least with the present magnification. Thus, the pH-sensitive behavior of {Con A/HRP}₅ films toward probes should be mainly attributed to the second mechanism and controlled by the electrostatic interaction between the films and the probe.

To further support this conclusion, other electroactive probes with a different charge situation than Fe(CN)₆³⁻, including positively charged Ru(NH₃)₆³⁺ and neutral FcOH, were investigated by CV at {Con A/HRP}₅ film electrodes in different pH buffers. For the Ru(NH₃)₆³⁺ probe, the pH-dependent CV switching behavior of the films was also observed, but the changing direction was opposite to that of Fe(CN)₆³⁻. At pH 9.0, Ru(NH₃)₆³⁺ showed a pair of well-defined and quasi-reversible CV peaks at about -0.20 V, with quite large peak heights for the films (Figure 10A, curve a). This is understandable since negatively charged films tended to attract positively charged Ru(NH₃)₆³⁺. However, in pH 4.0 solutions, this peak pair was greatly reduced (Figure 10A, curve b), which should be attributed to the electrostatic repulsion between positively charged films and Ru(NH₃)₆³⁺. In control experiments with bare PG electrodes, the CV response of Ru(NH₃)₆³⁺ in solution was pH-independent, suggesting that the pH-sensitive CV response of the probe at the film electrodes is not due to the property of the probe itself and must be related to the film property. Since the sizes of Fe(CN)₆³⁻ (6.0 Å) and Ru(NH₃)₆³⁺ (6.2 Å) are similar,³¹ the “opposite” pH-sensitive switching CV behavior of the films toward these two probes should be attributed to the different types of charges that they carry but not the pore size of the films, and the electrostatic interaction between the probe and the films should play a key role in deciding the direction of the pH-responsive on–off property.

For neutral probe FcOH, however, the pH-sensitive switching property for the films could not be observed. At both pH 4.0 and 9.0, a quasi-reversible redox peak pair of FcOH at about 0.20 V was observed at the {Con A/HRP}₅ film electrodes with very similar peak positions and heights (Figure 10B). This is understandable since FcOH carries no charge and there is no electrostatic interaction between the probe and the films. The alteration of film charge situation at different pHs cannot influence the diffusion of the neutral probe through the films by either electrostatic attraction or repulsion, thus leading to the similar peak heights at both pH 4.0 and 9.0. In control experiments, FcOH also showed a nearly reversible CV response at bare PG electrodes, which was pH-independent. These results confirm again that the electrostatic interactions between the {Con A/HRP}_n films and probes play a central role in deciding the pH-sensitive on–off behavior of the films toward the probes.

Conclusions

Mainly based on biospecific interaction between Con A and HRP, the {Con A/HRP}_n LbL films are successfully assembled on PG electrodes, and the glycoenzyme HRP is immobilized on the electrode surface. Since the films are stabilized mainly by the lectin–sugar rather than electrostatic interaction, the net film charge is easily modulated by the surrounding pH. In CV experiments with Fe(CN)₆^{3−} as the probe, the enzyme films are in the on state at pH 4.0 and in the off state at pH 9.0 and demonstrate a reversible pH-sensitive on–off switching property. The pH-dependent permeability of the system can be explained by electrostatic interaction between the films and the probe and is used to control the electrochemical reduction of H₂O₂ catalyzed by HRP in the films and mediated by Fe(CN)₆^{3−} in solution. To mimic the biological environment, the solution pH is modulated by in situ enzyme-catalyzed reactions and successfully used to stimulate the pH-sensitive bioelectrocatalysis of H₂O₂ with the same film–probe system. This system provides a novel model to control bioelectrocatalysis by immobilized enzyme through modulating the surrounding pH. The better understanding of the mechanism of the pH-sensitive switching behavior of this model system may also open a general way to develop new smart interfaces, which can be used as the foundation for fabricating pH-controllable biosensors based on bioelectrocatalysis with immobilized enzymes.

Acknowledgment. The financial support from the National Natural Science Foundation of China (NSFC 20975015 and 20775009) is acknowledged.

Supporting Information Available: Six figures showing CVs of Fe(CN)₆^{3−} at {Con A/HRP}_n film electrodes with different numbers of bilayers (*n*), dependence of the *I*_{pc} and Δ*E*_p of Fe(CN)₆^{3−} on the assembly step of {Con A/HRP}_n films, EIS responses of Fe(CN)₆^{3−/4−} for {Con A/HRP}_n films with different *n* and dependence of *R*_{ct} on *n* for {Con A/HRP}_n films, EIS responses of Fe(CN)₆^{3−/4−} for {Con A/HRP}₅ films at different pHs and dependence of *R*_{ct} on solution pH switched between pH 4.0 and 9.0, CVs of Fe(CN)₆^{3−} for {Con A/HRP}₄/Con A and {Con A/HRP}₅ films at different pHs, time-dependent pH changes generated by in situ enzyme-catalyzed reactions containing different concentrations of Est and Ur, and SEM top views of {Con A/HRP}₅ films after treatment with different pHs. This material is available free of charge via the Internet at <http://pubs.acs.org>.

References and Notes

- Rusling, J. F. *Acc. Chem. Res.* **1998**, *31*, 363.
- Chaubey, A.; Malhotra, B. D. *Biosens. Bioelectron.* **2002**, *17*, 441.
- Murphy, L. *Curr. Opin. Chem. Biol.* **2006**, *10*, 177.
- Pita, M.; Katz, E. *Electroanalysis* **2009**, *21*, 252.
- Willner, I. *Acc. Chem. Res.* **1997**, *30*, 347.
- Willner, I.; Katz, E. *Angew. Chem., Int. Ed.* **2000**, *39*, 1180.
- Tam, T. K.; Ornatska, M.; Pita, M.; Minko, S.; Katz, E. *J. Phys. Chem. C* **2008**, *112*, 8438.
- Tam, T. K.; Zhou, J.; Pita, M.; Ornatska, M.; Minko, S.; Katz, E. *J. Am. Chem. Soc.* **2008**, *130*, 10888.
- Yao, H.; Hu, N. *J. Phys. Chem. B* **2009**, *113*, 16021.
- Chaplin, M. F.; Bucke, C. *Enzyme Technology*; Cambridge University Press: Cambridge, U.K., 1990.
- Turner, A. P. F.; Karube, I.; Wilson, G. S. *Biosensors: Fundamentals and Applications*; Oxford University Press: New York, 1987.
- Decher, G. *Science* **1997**, *277*, 1232.
- Decher, G.; Schneloff, J. B. *Multilayer Thin Films: Sequential Assembly of Nanocomposite Materials*; Wiley-VCH: Weinheim, Germany, 2003.
- Lvov, Y.; Möhwald, H. *Protein Architecture: Interfacing Molecular Assemblies and Immobilization Biotechnology*; Marcel Dekker: New York, 2000.
- Hu, Y.; Hu, N. *J. Phys. Chem. B* **2008**, *112*, 9523.
- Lu, H.; Rusling, J. F.; Hu, N. *J. Phys. Chem. B* **2007**, *111*, 14378.
- Sultana, N.; Schenkman, J. B.; Rusling, J. F. *J. Am. Chem. Soc.* **2005**, *127*, 13460.
- Bourdillon, C.; Demaille, C.; Moiroux, J.; Saveant, J.-M. *J. Am. Chem. Soc.* **1994**, *116*, 10328.
- Anzai, J.; Takeshita, H.; Kobayashi, Y.; Osa, T.; Hoshi, T. *Anal. Chem.* **1998**, *2*, 811.
- Anzai, J.; Kobayashi, Y.; Nakamura, N.; Nishimura, M.; Hoshi, T. *Langmuir* **1999**, *15*, 221.
- Welch, K. T.; Turner, T. A.; Preast, C. E. *Bioorg. Med. Chem. Lett.* **2008**, *18*, 6573.
- Becker, J. W.; Reeke, G. N., Jr.; Cunningsham, B. A.; Edelman, G. M. *Nature* **1976**, *259*, 406.
- Anzai, J.; Kobayashi, Y. *Langmuir* **2000**, *16*, 2851.
- Katsuyama, T.; Spicer, S. S. *J. Histochem. Cytochem.* **1978**, *26*, 233.
- Liu, L.; Jin, X.; Yang, S.; Chen, Z.; Lin, X. *Biosens. Bioelectron.* **2007**, *22*, 3210.
- Liu, L.; Chen, Z.; Yang, S.; Jin, X.; Lin, X. *Sens. Actuators, B* **2008**, *129*, 218.
- Chen, Z.; Xi, F.; Yang, S.; Wu, Q.; Lin, X. *Sens. Actuators, B* **2008**, *130*, 900.
- Kobayashi, Y.; Anzai, J. *J. Electroanal. Chem.* **2001**, *507*, 250.
- Liu, Y.; Zhao, M.; Bergbreiter, D. E.; Crooks, R. M. *J. Am. Chem. Soc.* **1997**, *119*, 8720.
- Zhao, M.; Liu, Y.; Crooks, R. M.; Bergbreiter, D. E. *J. Am. Chem. Soc.* **1999**, *121*, 923.
- Park, M.-K.; Deng, S.; Advincula, R. C. *J. Am. Chem. Soc.* **2004**, *126*, 13723.
- Kang, E.; Liu, X.; Sun, J.; Shen, J. *Langmuir* **2006**, *22*, 7894.
- Karyakin, A. A.; Gitelmacher, O. V.; Karyakina, E. E. *Anal. Chem.* **1995**, *67*, 2419.
- Ben-Naim, A. Y. *Cooperativity and Regulation in Biochemical Processes*; Springer: Berlin, Germany, 2001.
- Katz, E.; Pita, M. *Chem. Am. Eur. J.* **2009**, *15*, 12554.
- Amir, L.; Tam, T. K.; Pita, M.; Meijler, M. M.; Alfonsa, L.; Katz, E. *J. Am. Chem. Soc.* **2009**, *131*, 826.
- Zhou, J.; Tam, T. K.; Pita, M.; Ornatska, M.; Minko, S.; Katz, E. *ACS Appl. Mater. Interfaces* **2009**, *1*, 144.
- Yao, H.; Guo, X.; Hu, N. *Electrochim. Acta* **2009**, *54*, 7330.
- Denuziere, A.; Ferrier, D.; Domard, A. *Carbohydr. Polym.* **1996**, *29*, 317.
- Hill, H. A. O. *Pure Appl. Chem.* **1987**, *59*, 743.
- Lvov, Y.; Ariga, K.; Ichinose, I.; Kunitake, T. *Thin Solid Films* **1996**, *284/285*, 797.
- Welinder, K. G. *Eur. J. Biochem.* **1979**, *96*, 483.
- Ferri, T.; Poscia, A.; Santucci, R. *Bioelectrochem. Bioenerg.* **1998**, *44*, 177.
- Huang, R.; Hu, N. *Biophys. Chem.* **2003**, *104*, 199.
- Murray, R. W. *Electroanalytical Chemistry*; Bard, A. J., Ed.; Marcel Dekker: New York, 1984; Vol. 13, pp 191–368.
- Volodkin, D. V.; Larionova, N. I.; Sukhorukov, G. B. *Biomacromolecules* **2004**, *5*, 1962.
- Pan, S.; Arnold, M. A. *Anal. Chim. Acta* **1993**, *283*, 663.
- Li, W.; Yuan, R.; Chai, Y.; Zhou, L.; Chen, S.; Li, N. *J. Biochem. Biophys. Methods* **2008**, *70*, 830.
- Lu, B.; Smyth, M. R.; Quinn, J.; Bogan, D.; O’Kennedy, R. *Electroanalysis* **1996**, *8*, 619.
- Ruzgas, T.; Csoregi, E.; Emneus, J.; Gorton, L.; Marko-Varga, G. *Anal. Chim. Acta* **1996**, *330*, 123.
- Jencks, W. P. *Catalysis in Chemistry and Enzymology*; Dover: New York, 1987.
- Kokufuta, E.; Tanaka, T. *Macromolecules* **1991**, *24*, 1605.
- Estiu, G.; Merz, K. M., Jr. *J. Am. Chem. Soc.* **2004**, *126*, 6932.
- Motornov, M.; Sheparovych, R.; Katz, E.; Minko, S. *ACS Nano* **2008**, *2*, 41.
- Antipova, A. A.; Sukhorukov, G. B. *Adv. Colloid Interface Sci.* **2004**, *111*, 49.
- Calvo, A.; Yameen, B.; Williams, F. J.; Soler-Illia, G. J.; Azzaroni, O. *J. Am. Chem. Soc.* **2009**, *131*, 10866.